Analytical Methods

Accepted Manuscript

This article can be cited before page numbers have been issued, to do this please use: K. Hu, J. Cheng, J. Li, S. Ye, H. Yang, Y. Liu and J. Kong, *Anal. Methods*, 2020, DOI: 10.1039/D0AY00328J.

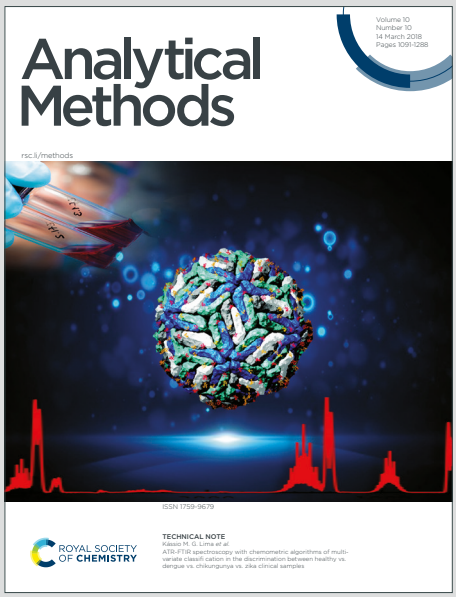

ROYAL SOCIETY OF CHEMISTRY

rsc.li/methods

DOI: 10.1039/D0AY00328J

Perfluorosulfonic acid polymer based eATRP for ultrasensitive detection of CYFRA21-1 DNA

Received 00th January 20xx,
Accepted 00th January 20xx

DOI: 10.1039/x0xx00000x

Kai Hu[a], Jiamin Cheng[a], Jinge Li[a], Shan Ye[a], Huaixia Yang[a, *], Yanju Liu[a, *],

Jinming Kong[b, *]

The sensitive detection of biomarker cytokeratin fragment antigen 21-1 (CYFRA21-1) is crucial for early diagnosis and screening of non-small cell lung cancer (NSCLC). In this work, an electrochemical biosensor based on Nafion-initiated eATRP has been built for ultrasensitive detection of CYFRA21-1 DNA for the first time. Specifically, the peptide nucleic acid (PNA) probes are immobilized onto the gold electrode surface, then hybridize with target DNA to form PNA/DNA heteroduplexes for the subsequent attachment of Nafion by the identified carboxyl-Zr^{4+}-phosphoric acid chemistry. Finally, polymer chains are obtained by linking the monomer of ferrocenylmethyl methacrylate to the PNA/MCH/DNA/Zr^{4+}/Nafion probes via eATRP. Under optimized steady-state conditions, the sensor offers a wide current response for CYFRA21-1 DNA from 10^{-11} to 10^{-16} M with a detection limit of 6.42×10^{-17} M. The proposed method of using Nafion as the eATRP initiator exhibits high sensitivity, reproducibility and stability, is a promising strategy for early diagnosis of NSCLC.

Introduction

Lung cancer, with a similar incidence and mortality, is one of the highest incidence common malignant tumors in the world [1]. Lung cancer is classified as non-small cell lung cancer (NSCLC) and small cell lung cancer (SCLC) [2]. NSCLC which accounts the majority of lung cancer cases is commonly managed with chemotherapy and radiation therapies, while SCLC is usually treated surgically. Once the cancer has been diagnosed, the patient's survival rate is very low, so it is most important to diagnose the disease at an early stage [3]. Hence, many methods have been developed, including chest radiography [4], positron emission tomography [5], biopsies [6], computed tomography [7], magnetic resonance imaging [8] and sputum cytology [9]. However, the above methods are not suitable for all patients due to the various types of pathology involved [10]. Many studies revealed that the content of CYFRA21-1 is closely related to the status of NSCLC [11]. Therefore, the CYFRA21-1 DNA is considered to be one of the most important diagnostic biomarkers of NSCLC [6,12]. Many techniques have been previously developed to detect cancer based on specific DNA sequences, including western blot, and reverse transcriptase-polymerase chain reaction (RT-PCR) [13,14]. However, these techniques have limitations because some of them are time-consuming, imprecise, technically difficult and expensive. Hence, development of a fast, sensitive, simple operation clinical assay for the detection of CYFRA21-1 DNA is urgently needed.

Currently, owing to the advantages of high specificity and sensitivity, rapid response, and low-cost, the electrochemical biosensing of DNA has already successfully used for the ultrasensitive detection of low molecular level biomarkers [15-17]. To further improve the sensitivity of the biosensors, different types of polymerization reactions and nanomaterials have been used for DNA detection, such as electrochemically mediated atom transfer radical polymerization (eATRP) [18], photopolymerization [19], AuNPs [20]. Compared to other methods, eATRP is a robust and effective measure for the preparation polymeric materials with controlled molecular weights and well-defined architectures [21,22]. Recently, Sun et al. reported a DNA biosensor, which was successfully used for the detection of target DNA (tDNA) in standard serum samples, based on eATRP signal amplification and "Click Chemistry" [18]. This expanded the prospect of the developed DNA biosensor in the detection of gene biomarkers, but as noted, the development of an

[a] Henan University of Chinese Medicine, Zhengzhou 450046, P. R. China E-mail: yhx998@hactcm. edu.cn; liuyanju886@hactcm.edu.cn
[b] School of Environmental and Biological Engineering, Nanjing University of Science and Technology, Nanjing 210094, P. R. China E-mail: j.kong@njust.edu.cn

View Article Online
DOI: 10.1039/D0AY00328J

eATRP amplification strategy for the detection of trace level tDNA is still urgently required.

Nafion is a kind of perfluorosulfonic acids (PFSA) polymer formed by free radical polymerization of perfluorovinyl ether sulfonyl fluoride comonomer with tetrafluoroethylene (TFE). It is widely used in organic catalysis, environmental protection and proton exchange membrane for fuel cell [23,24]. In particular, Nafion has the advantages of easy separation, recovery and regeneration [25-27]. Based on the properties and advantages of Nafion, the mechanism of Nafion as initiator in this experiment is the same as that of alkyl halide (RX) as initiator. The sulfonic acid groups in the side chains of the polymers are inherently reactive sites of this copolymer, and some C-F groups with low bond dissociation energies (BDE) backbone are potentially active sites to initiate the eATRP reaction [28]. Recently, Peng et al. have confirmed for the first time that the C-F group on the Nafion can be used as the active sites of the macromolecular initiator for ATRP [25]. Compared with other initiators, Nafion has more active sites and is more stable in the aqueous phase [25,29]. It is worth noting that as the initiator of eATRP, it can provide a new window for the design of PFSA via the eATRP reaction, which has great potential in signal amplification. Moreover, there are few studies on constructing sensors for detection of trace DNA by combining Nafion with eATRP reactions. Therefore, an electrochemical biosensor has been built based on Nafion-initiated eATRP for ultrasensitive detection of CYFRA21-1 DNA for the first time.

The sequential preparation of the electrochemical DNA biosensor is illustrated in Scheme 1. PNA can be used as a high-specific probe for the detection of ssDNA and dsDNA, because it can specifically recognize and bind to its complementary target [30]. Herein, PNAs are immobilized onto the gold electrode surface via Au-S bond and hybridize with tDNA forming PNA/DNA heteroduplexes. Then, the eATRP initiator of Nafion is attached to the heteroduplexes by phosphate-Zr^{4+}-sulfosalt chemistry, because Zr^{4+} can form stable conjugates with the sulfonic acid group of Nafion and the phosphate groups of PNA/DNA heteroduplexes through strong coordination interactions. Finally, the electroactive probes are obtained after labeling of ferrocenylmethyl methacrylate (FMMA) via eATRP. The combination of using the eATRP polymerization as a signal amplification strategy with Nafion as a macroinitiator achieves a good amplification effect, and also has promise for the detection of trace DNA.

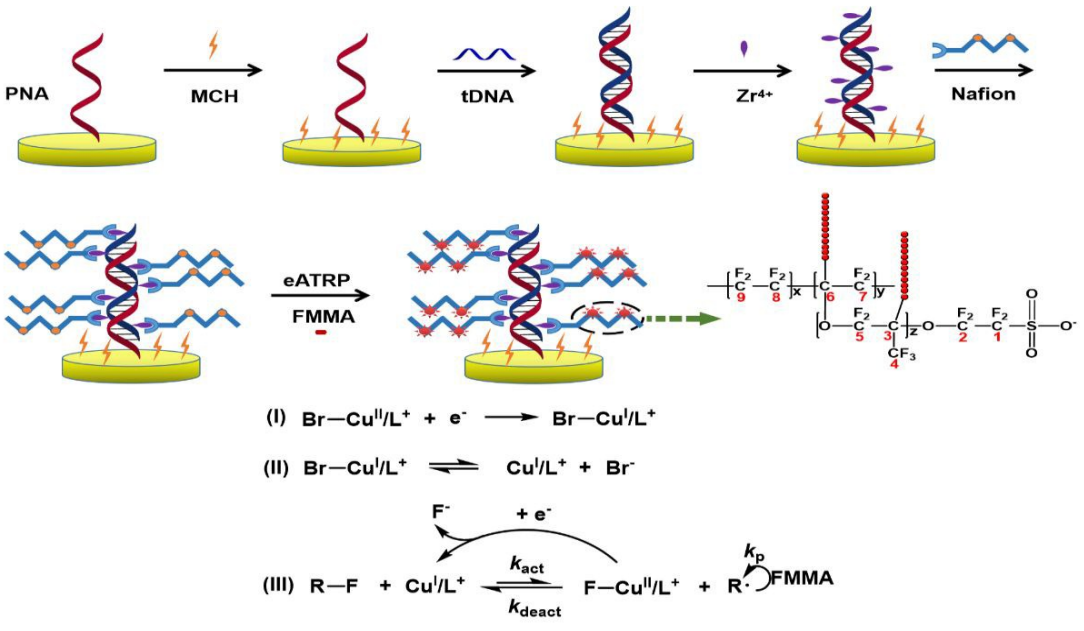

View Article Online
DOI: 10.1039/D0AY00328J

Scheme 1 Illustration of the preparation of electrochemical DNA biosensor based on eATRP

Experimental section

Chemicals and materials

Thiolated PNA was designed by Panagene Inc. (South Korea). All the sequence of ssDNA was synthesized by Sangon Biotech (Shanghai) Co., Ltd, including target DNA (tDNA), single-base mismatched DNA (SBM), three bases mismatched DNA (TBM), and control DNA (Control) is non-complementary DNA. Their sequences were listed in **Table 1**. 6-mercapto-1-hexanol (MCH), normal human serum (NHS) and Nafion (Nafion® 117, W/V 5.2%) were provided by Sigma-Aldrich (Shanghai) Trading Co., Ltd. (Shanghai, China). Ferrocenylmethyl methacrylate (FMMA) was provided by Bide Pharmatech Ltd. (Shanghai, China). Tris(2-dimethylaminoethyl) amine (Me_6TREN) was got from Aladdin Reagent (Shanghai, China) Co., Ltd. Lithium perchlorate trihydrate ($LiClO_4 \cdot 3H_2O$), potassium hexafluorophosphate (KPF_6) and Zirconium dichloride oxide octahydrate ($ZrOCl_2 \cdot 8H_2O$) were gained from J & K Scientific Ltd. (Shanghai, China). N, N-dimethylformamide (DMF) and copper (II) bromide ($CuBr_2$) were obtained from Sinopharm Chemical Reagent Co., Ltd. (Shanghai, China). All other reagents were of analytical grade unless otherwise stated.

Phosphate buffer saline (PBS, 0.1 M) was prepared by mixing NaH_2PO_4 and Na_2HPO_4 solutions at room temperature (pH 7.4). The tDNA solution of different concentrations was dilution with PBS. Dissolve the $CuBr_2$ and Me_6TREN into DMF for making $Cu^{II}Br/Me_6$TREN complexes (10 mM). ''Piranha'' solution was prepared by using 30% H_2O_2 and 98% H_2SO_4 at 1:3 volume ratio (Please take care of safety in its preparation because the solution is strongly acidic and has corrosive power). The eATRP mixture (pH 7.0) was made up a variety of freshly prepared mixtures: including DMF (1.8 mL), $Cu^{II}Br/Me_6$TREN (0.1 mL, 10 mM), FMMA (0.1 mL, 10 mM, dissolved in DMF), KBr (1 M, 1.0 M), KPF_6 (7.0 mL, 0.1 M).

Table 1 Sequences of PNA and ssDNAs.

Synthetic oligonucleotide	Base sequences (5'-3')
tDNA	CGCCCCTGACACCATTCCTCCCTTC
SBM	CGCCCCTAACACCATTCCTCCCTTC
TBM	CGCCCATGACACTATTCCTCGCTTC
Control DNA (Control)	TATTATCCGTCAGTGGAAAGGACCG
PNA	SH-$(CH_2)_{11}$-(O linker)$_3$-GAAGGGAGGAATGGTGTCAGGGGCG

Apparatus

Electrochemical impedance spectroscopy (EIS), cyclic voltammogram (CV), linear sweep voltammetry (LSV) and square wave voltammetry (SWV), were accomplished with the Autolab/MAC90179 electrochemical workstation (Eco Chemie, Netherlands). The three electrodes of classical electrode system were made of gold (2 mm in diameter), calomel and platinum. Atomic force microscopy (AFM) measurements were acquired with Bruker Dimension Icon instrument.

Construction of electrochemical biosensing

In general, the gold electrodes were cleaned in a two-step operation: the electrodes were continuously polished with very fine alumina slurries on the suede for reaching the mirror, and then cleaned by anhydrous ethanol and ultrapure water. The polished electrodes were soaked in the newly prepared ''Piranha'' solution for 15 min and, the electrodes were immediately treated with CV in 0.5 M H_2SO_4 solution until a repetitive cyclic voltammogram was obtained. The range of potential was set at -0.3~1.5 V, with a scanning rate of 0.1 Vs^{-1}. Subsequently, EIS was applied to the bare electrodes in 5.0 mM $[Fe(CN)_6]^{4-/3-}$ solution to measure the resistance after each step of the operation [31]. Finally, the electrodes were washed with ultra-pure water and dried with N_2.

View Article Online
DOI: 10.1039/D0AY00328J

PNA/MCH/tDNA/Zr^{4+}-modified electrodes were prepared as follows. Firstly, the PNA (5.0 μL, 0.5 μM) solution was dropped onto the electrodes and placed overnight at room temperature to immobilize the capture probe. After washing with ultrapure water, the modified electrodes were soaked in 2.0 mM MCH (60% EtOH) for 30 min, in order to occupy the rest of the active sites to prepare for the successful crossing between PNA and DNA, and then washed with 60% EtOH and water. Then the tDNA (10 μL, 0.1 nM) was pipetted onto the electrodes, followed by incubation at 37 °C for 1.5 h, and rinsed with 0.1 M PBS to remove unbound tDNA molecules. Finally, the electrodes were dipped in $ZrOCl_2$ (5.0 mM, dissolved in 10% EtOH) at 37 °C for 15 min, and then washed with 10% EtOH.

Electrodes modified with PNA/MCH/tDNA/Zr^{4+}/Nafion/FMMA were obtained by the following steps. The Nafion solution (5 μL, 5.2% W/V) was added onto the as-preparaed electrodes for the attachment to PNA/DNA heteroduplexes at 37 °C for 40 min, then the electrodes were washed with ultrapure water. Next, the prepared electrodes were immersed in an eATRP mixed solution. $Cu^{II}Br/Me_6TREN$ was electrochemically reduced to Cu^{I}/Me_6TREN at a constant potential (E_{app}), then all electrodes were rinsed with DMF and water immediately after treatment with LSV (0~0.2 V, scanning rate: 1.0 Vs^{-1}) to remove Cu which may be generated by Cu^{+}. Finally, the electrochemical signal was obtained by packing the electrodes into 1.0 M $LiClO_4$, and the SWV (0~0.6 V, increase potential: 4.0 mV s^{-1}; potential amplitude: 25 mV) was actualized.

Results and discussion

The principle of Nafion-initiated eATRP

In Scheme 1, the theory of eATRP amplification with Nafion as the initiator was illustrated. Me_6TREN is a commonly branch tetracentate ligand which can be used to fill the coordination shell of copper ion in copper-mediated ATRP reaction [28]. In the first and second steps, $Cu^{II}Br/L^{+}$ was reduced to $Cu^{I}Br/L$ under the E_{app} (L represents Me_6TREN), the latter $Cu^{I}Br/L$ dissociated to Cu^{I}/L^{+} and Br^{-}. In the third step, Cu^{I}/L^{+} as the activator reacted with initiators producing the initiating radicals (R·) and $Cu^{II}F/L^{+}$ deactivators. Then R· and FMMA were reacted to produce free radical R-FMMA·. The reaction of R-FMMA· with $Cu^{II}F/L^{+}$ resulted in the target product R-FMMA-F, and the transition metal was reduced to Cu^{I}/L^{+}, and then a new round of reaction can be initiated again. Afterwards, amount of FMMA molecules was reacted with R· to amplify the signal successfully. Because the reaction is a rapid equilibrium reaction, the formation of R-R group leads to the termination of the reaction when the concentration of R· is high. In order to avoid premature termination of the reaction and keep the concentration of R· at a low level, so $k_{act} << k_{deact}$ in the equation, and the numerical change of k_{act} is closely related to initiator and catalytic system when k_{deact} is stable at a larger value. Meanwhile, K_{ATRP} represents the ATRP equilibrium constant and k_p represents the rate constant of monomer polymerization in the Eq. (1, 2). K_{ATRP} is related to the polymerization rate R_P and the concentration of R· [32,33]. In turn, in order to obtain higher K_{ATRP}, increasing the value of k_{act} as much as possible, numerous monomers are gathered on the electrode surface.

$$K_{ATRP} = \frac{k_{act}}{k_{deact}} \quad \text{Eq. 1}$$

$$R_p = k_p C_M C_R = k_p C_M K_{ATRP} C_{RX} \frac{C_{Cu^I}}{C_{Cu^{II}}} \quad \text{Eq. 2}$$

Briefly, eATRP technology is suitable for controllable polymerization of large amounts of monomers, and the core of the technology is the use of initiators. The speed of initiation has an important impact on the formation of well-defined polymers, and the amount and structure of the initiator play an important role in the conversion rate of the monomer and formation of the polymer chain. In the course of the reaction, C-F bonds of Nafion were broken leading to the R· and the F^{-}, F^{-} was captured by Cu+ which was reduced from Cu^{2+} under the E_{app}. The whole catalytic system can be used as a carrier of F^{-}, and a reversible dynamic equilibrium

View Article Online
DOI: 10.1039/D0AY00328J

between living species and dormant species is established by a redox reaction. In previous studies, the position of active sites was determined by comparing the normalization peak area of the C-F bond on the Nafion chain before and after the eATRP reaction, using their ^{19}F NMR spectra [25,27]. The available data showed that the bond energy of C3-F group on the side chain was slightly lower than that of the C6-F group on the main chain, and it was the lowest in the whole chain. These two active sites have been confirmed by different groups. As noted, C1-F, C2-F, C4-F, C5-F, C8-F were also found to be the potentially active sites [25,26,34]. When C8-F_2 is converted to C8-F, the bond energy of C8-F is equal to that of C6-F, and so it is an active site. In Scheme 1, there are a large number of active sites in the Nafion chain, which means that it has great advantages over the initiator of an active site. However, most of the eATRP initiators used C-Cl or C-Br as the active group, and in contrast, the use of C-F bonds is minor. Because the bond energy of C-F bond is stronger than that of C-Cl and C-Br, resulting in a slower reaction rate [35].

AFM characterization

Fig. S1 presented the AFM phase images of the PNA/MCH/tDNA/Zr^{4+}/Nafion-modified electrode and PNA/MCH/tDNA/Zr^{4+}/Nafion/FMMA-modified electrode. The surface of the former with heights exceeding 45.8 nm which was higher than the latter due to the formation height of the polymer. The rms roughness measures were 4.18 nm and 2.64 nm, respectively. This result implies the formation of the polymer chain on the electrode.

Electrochemical characterizations

Prior to the eATRP polymerization, the E_{app} was examined by CV in the FMMA-free eATRP cocktail with the modified electrode before the eATRP. As can be seen in **Fig. S2**, the optimal E_{app} was selected at -0.5 V vs SCE, which the potential of reduction peak when $Cu^{II}Br/Me_6TREN$ was reduced to $Cu^{I}Br/Me_6TREN$ [35].

In order to verify the feasibility of this electrochemical biosensor using the Nafion as the initiator, different SWV signal were shown in **Fig.1A**. The curves (a)-(f) in the figure reflected the absence of any significant oxidation current appearing when PNA, DNA, Zr^{4+}, Nafion, FMMA, and $Cu^{II}Br/Me_6TREN$ were not added during the experiment. When all the components were added the current (g) showed an intense oxidation and the potential corresponding to the peak value was 0.35 V (*vs* SCE) after the eATRP polymerization. This anodic peak caused by the oxidation of ferrocene into ferrocenium, is in the typical range of ferrocene redox potentials [36]. These results demonstrated that the lack of any component in the electrodes leads to an unsuccessful modification, and the eATRP-based electrochemical biosensor could be used for detecting trace DNA fragment as a signal amplification strategy. Therefore, all these tests proved the feasibility and reliability of the proposed method.

After the eATRP reaction, CV was applied to characterize the electrodes modified with newly formed electroactive polymer at different scan rates. The linear relationship between redox current and scan rate was good in **Fig. 1B**, indicating that electroactive polymers were covalent immobilized rather than diffusion dependent. The poor reversibility of CVs could also be observed, and was probably due to the fact that polymer chains hinder the electron transfer between the electrode surface and the solution.

The modified electrodes in the sequential preparation process were investigated by CV and EIS in 5.0 mM $[Fe(CN)_6]^{4-/3-}$ solution containing 0.1 M KNO_3. The changes of current and resistance were compared to observe the modification of electrodes surface (**Fig. 1C**; **Fig.1D**). In EIS, the semicircle of impedance curves corresponding to the surface electron-transfer resistance (R_{ct}) in the high frequency region [37,38].The

View Article Online
DOI: 10.1039/D0AY00328J

bare gold electrodes exhibited a couple of reversible redox peaks of $[Fe(CN)_6]^{4-/3-}$ at a scan rate of 100 mV·s^{-1} and a very small R_{ct} of 193 Ω, which reflected the electrodes were clean and had good electrical conductivity (curve a). After modification with PNA, redox intensity decreased, suggesting that the effective area was reduced and the electron transfer was inhibited (curve b). When MCH was added to the surface, other nonspecific sites were covered, resulting in CV responses was decreased again (curve c). More negative charges were introduced through tDNA probes, which hindered electron transfer and the redox intensity further decreased (curve d). With the introduction of Zr^{4+}, the peak current further decreased (curve e). The resistance increased continuously with the formation of PNA/MCH/DNA/Zr^{4+} probes (~290 Ω, curve b; ~384 Ω, curve c; ~1050 Ω; curve d; ~1.70 kΩ; curve e). Subsequently, Nafion were introduced, resulting in CV response decreased significantly and the peak value of current response about 5 μA, with a significant increase in the R_{ct} (7.4 kΩ, curve f). Finally, FMMA was modified to the electrodes by ATRP reaction, due to the conductivity of FMMA which facilitated the electronic transfer of the interface, the current value was much higher than PNA/MCH/DNA/Zr^{4+}/Nafion modified electrodes, meanwhile the impedance value was significantly reduced after the eATRP amplification compared to the last step (~4.4 kΩ; curve g), indicating the successful labeling of FMMA. All the impedance curves could be superimposed, and the resistance was gradually increased on the whole, proving the authenticity of this reaction.

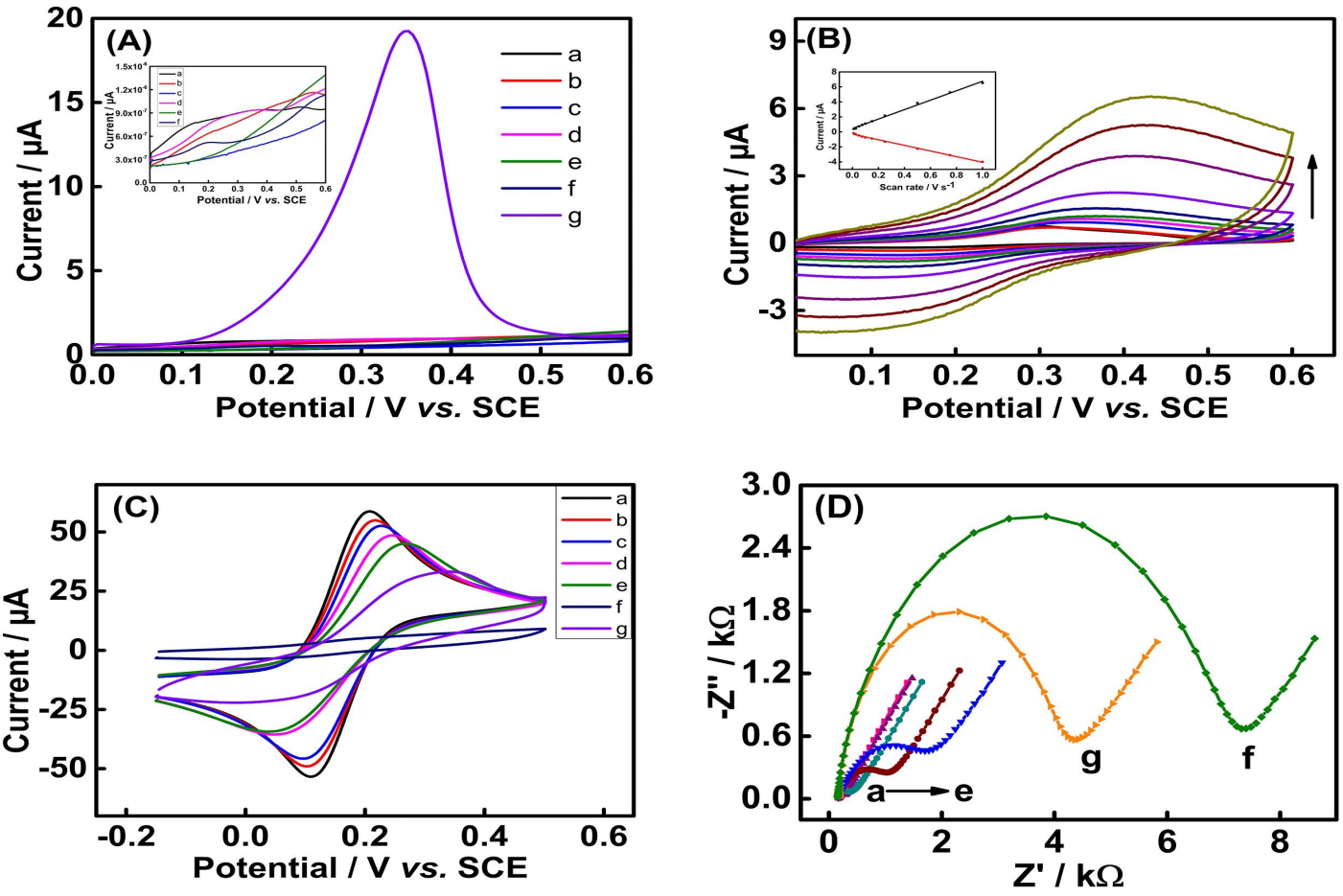

View Article Online
DOI: 10.1039/D0AY00328J

Fig.1 (A) The square wave voltammogram of the PNA/MCH/DNA/Zr^{4+}/Nafion/FMMA-modified electrode (g), and others curves without PNA (a), MCH (b), tDNA (c), Zr^{4+} (d), Nafion (e), FMMA (f). (B) The cyclic voltammogram of the PNA/MCH/DNA /Zr^{4+}/Nafion/FMMA-modified electrode in 0.5 M $LiClO_4$ at different scan rates from 10 to 1000 mV s^{-1}. Inset: The linear relationship between anodic and cathodic peak currents and scan rate. (C) a Cyclic voltammograms and (D) Nyquist plots of the electrochemical impedance spectroscopy (EIS) for stepwise assembling process of the electrode in 5.0 mM $[Fe(CN)_6]^{4-/3-}$ solution containing 0.1 M KNO_3. The results are shown in the figures, the bare gold electrode (a), PNA (b), PNA/MCH (c), PNA/MCH/DNA (d), PNA/MCH/DNA/Zr^{4+} (e), PNA/MCH/DNA/Zr^{4+}/Nafion (f), PNA/MCH/DNA/Zr^{4+}/Nafion/ FMMA (g) modified gold electrode. The concentration of tDNA was 1 pM. The eATRP time was 40 min.

Optimization of conditions

It is of paramount importance to select the best process conditions. In this section, the three key factors including initiator reaction time, the pH of the eATRP cocktail and eATRP time were studied.

In the eATRP, Nafion contained multiple C-F bonds which produced multiple R· and F^- ions, and were based on the transfer of halogen atoms in the experiment. The polymerization reaction was controlled effectively via a reversible dynamic equilibrium between the F^- and R-F. With a good initiator, initiation should be fast and steady. As can be seen in **Fig. S3A**, the current value increased significantly in the first 15 min, but the current value was almost kept constant for the subsequent 15 min. Therefore, the optimal reaction time of initiator was selected as 15 min.

According to previous studies, the most suitable pH for the eATRP reaction was 7.0 [39]. The dissociation of the complex and the disproportionation of Cu^{I} took place at low pH, and at high pH, the OH^- ions would compete with F^- for combination with Cu^{II}. In the eATRP cocktail, the more polymerization time can ensure that the numerous FMMA was assembled onto the electrode surface, thus polymer chains grew longer. In order to ascertain the optimal aggregation time, CV was conducted to monitor the growth process of polymers. Figs. **S3B** and **S3C** revealed the dynamic process of eATRP polymerization. As suggested in these Figures, the peak current increases with the increase of polymerization time, and the current value remains stable at 40 min. so the polymerization time was selected at 40 min. This phenomenon was owing to the effect of steric hindrance from the long polymer chain which the molecular weight of Nafion is high.

Analytical performance

In this experiment, the concentration of tDNA was changed from 0.1 fM to 10 pM to obtain the incremental response values of SWV. As shown in **Fig. 2A**, increasing oxidation peaks appeared at a potential of 0.35 V *vs* SCE. Good linear relationship between the SWV response and the logarithm of tDNA concentration was shown in **Fig. 2B**. The linear regression equation was I (μA) = 10.66 + 2.11 log [C_{tDNA}/pM] (R^2 = 0.997), and the limit of detection (LOD) was 6.42 ×10^{-17} M (C_{LOD} = *3σ/slope, σ* represent the standard deviation of the control). Apparently, the LOD was much lower than the reported strategies [36,40-42], as summarized in **Table 2**. The initiator can combine with FMMA and produce a number of electroactive probes via eATRP, and this effectively improved the electrochemical signal greatly at lower cost and in a shorter time. All these results confirmed the feasibility and validity of Nafion as an initiator.

Table 2 Comparison of this method with others detection of DNA

Amplification strategy	L. R. (M)	D.L. (M)	probe	refs
Electrochemical	6×10^{-10}-2.1×10^{-3}	0.5×10^{-9}	hairpin DNA	36
Electrochemical	1×10^{-12}-1×10^{-9}	5.34×10^{-12}	PNA	42
Fluorometric	1×10^{-10}-	3×10^{-12}	CdS	40

View Article Online
DOI: 10.1039/D0AY00328J

	1×10^{-9}		quantum dot (QD)		chemiluminescence	1×10^{-16}-1×10^{-12}	4×10^{-16}	PNA	44
Fluorometric	1×10^{-12}-1×10^{-9}	2.96×10^{-13}	hairpin DNA	43	Electrochemical	1×10^{-16}-1×10^{-11}	6.42×10^{-17}	PNA	this work

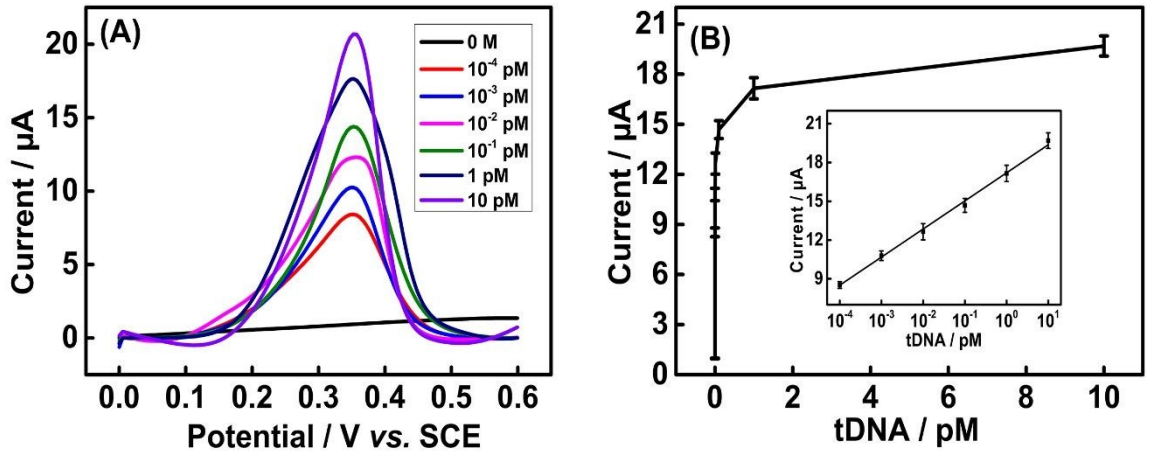

Fig.2 (A) The square wave voltammograms of PNA/MCH/DNA/Zr^{4+}/Nafion/FMMA-modified electrode toward different concentrations of tDNA over the range of 0.1 fM to 10 pM. (B) Corresponding calibration curve. Error bars show the SDs of four independent assays.

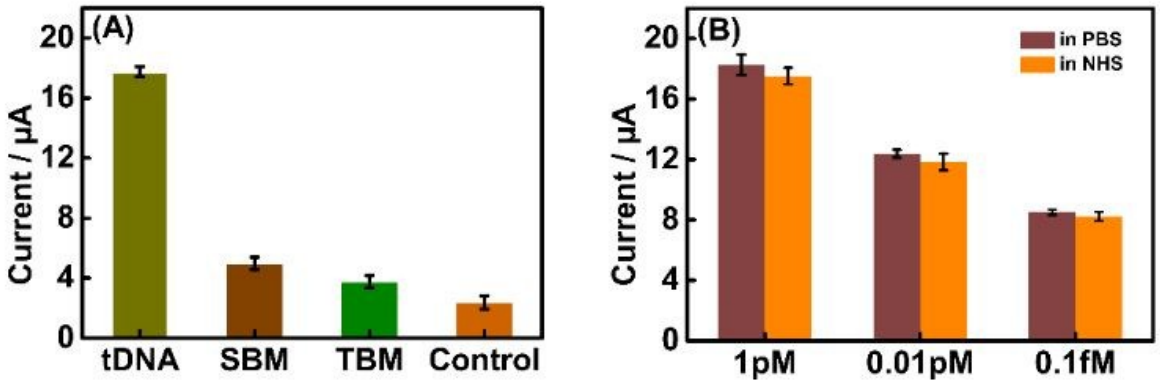

Fig.3 (A) SWV responses toward 1 pM tDNA, SBM, TBM, and Control. (B) SWV responses toward 1 pM tDNA in PBS, 5% serum sample.

Stability, reproducibility, selectivity and anti-interference capacity

The modified electrodes after eATRP were stored at 4 °C for testing the stability of our strategy. Two sets of electrodes (24 for each set) were prepared under the same conditions. One group was immediately measured with SWV after preparation, and the electrodes of the other group were stored in a refrigerator at 4°C. Two electrodes were tested every two days. Of note, up to 94.25% of the current signal can be retained for 18 days with a relative standard deviation (RSD) of 1.99%, indicating the desirable stability of this strategy.

Further, the reproducibility of this method for eATRP amplification with Nafion as initiator was evaluated with the intra-assays and inter-assays. The variation coefficients of the intra-assay and inter-assay were 2.49% and 2.88% (n=5), respectively, indicating that the method had highly reproducibility.

When the selectivity of our method was tested with SWV, there was an obvious signal difference between the tDNA and the other three kinds of DNA, including

View Article Online
DOI: 10.1039/D0AY00328J

SBM, TBM, and Control. As can be seen from **Fig. 3A.** there was an obvious signal difference between the tDNA and the other three kinds of DNA, including SBM, TBM, and Control. The current intensities from SBM, TBM, and Control were approximately 27.97%, 21.24%, and 13.38% of the value from tDNA, respectively. The high selectivity of this strategy can be attributed to the favorable immunity associated with the elimination of background current of SWV, as well as the excellent specificity of PNA probes.

SWV was applied to assess the application potential and feasibility of this strategy in NHS. A contrasting analysis of oxidation current values of tDNA samples that diluted with 0.1M PBS or 5% NHS was obtained and shown in **Fig. 3B**. As can be seen, the recovery values of different concentration of tDNA from 5% NHS samples values were 95.90%, 95.66% and 96.74%, respectively. In addition, tDNA samples of different concentrations with whole serum were prepared. Their electrochemical responses were compared with these of PBS. However, the results were not satisfactory. The reason may be that although the sensitivity of electrochemical sensor is very high, its anti-interference ability is limited. Therefore, it is necessary to continuously develop and improve it in order to promote its clinical application.

Conclusions

We reported a fire-new and ultrasensitive electrochemical DNA biosensor for detection of low concentration of DNA molecules, by exploiting Nafion as a macroinitiator and eATRP polymerization as a signal amplification strategy. Nafion was selected as an efficient initiator that can unite numerous monomers by linking to each phosphorylated site, resulting in the formation of polymerization chains and achieving significant amplification. Therefore, this strategy had an extremely low LOD, high selectivity and satisfactory stability even in complex NHS conditions. Additionally, it showed simple operation, labor- and time-saving results, and excellent specificity. More importantly, different Nafion derivatives can be formed by the combination of PFSA polymer with ATRP polymerization, which could extend its structural types and field of application. All of these observations suggest the great potential of this method in clinical applications.

Conflicts of interest

There are no conflicts of interest to declare.

Compliance with Ethics Requirements

This article does not contain any studies with human or animal subjects.

Acknowledgements

This study was financially supported by National Natural Science Foundation of China (21605042, 21974068); Key Science and Technology Research Project of Henan Province (192102310033, 182102310257).

References

1. A. Jemal, F. Bray, M. M. Center, J. Ferlay, E. Ward and D. Forman, *Ca-Cancer J. Clin*, 2011, **61**, 69-90.
2. L. Ferrer, M. G. Levra, M. Brevet, M. Antoine, J. Mazieres, G. Rossi, R. Chiari, V. Westeel, M. Poudenx, J. Letreut, R. Gervais, G. Osman, N. Girard, A. C. Toffart, S. Novello and D. Moro-Sibilot, *J. Thorac. Oncol.*, 2019, **14**, 130-134.
3. N. A. Pennell, J. W. Neal, J. E. Chaft, C. G. Azzoli, P. A. Janne, R. Govindan, T. L. Evans, D. B. Costa, H. A. Wakelee, R. S. Heist, M. A. Shapiro, A. Muzikansky, S. Murthy, M. Lanuti, V. W. Rusch, M. G. Kris and L. V. Sequist, *J. Thorac. Oncol.*, 2019, **37**, 97.
4. D.R. Aberle, A.M. Adams, C.D. Berg, W.C. Black, J.D. Clapp, R.M. Fagerstrom, I. F. Gareen, C. Gatsonis, P. M. Marcus, J. D. Sicks, *N. Engl. J. Med* 2011, **365**, 395-409.
5. J.H. Kim, Y.H. Joo, Y.D. Son, J.H. Kim, Y.K. Kim, H.K. Kim, S.Y. Lee and T. Ido, *Eur. Neuropsychopharmacol.*, 2019, **29**, 278-290.
6. M. Chen, Y. Y. Wang, H. L. Su, L. Mao, X. N. Jiang, T. Zhang and X. Z. Dai, *Sens. Actuators, B*, 2018, **255**, 2910-2918.
7. C. I. Henschke, R. Yip, D. F. Yankelevitz and J. P. Smith, *Ann. Intern. Med.*, 2013, **159**, 156-157.
8. M. J. Betts, A. Cardenas-Blanco, M. Kanowski, A. Spottke, S. J. Teipel, I. Kilimann, F. Jessen and E. Duzel, *Alzheimer's dementia*, 2019, **11**, 281-285.
9. N. Belachew, S. Jerkic, F. Michel, R. Schubert, S. Zielen and M. Rosewich, *Pneumologie*, 2019, **73**, 399-406.
10. L. L. Wang, *Sensors*, 2017, **19**.

DOI: 10.1039/D0AY00328J

11. Z. Altintas and I. Tothill, *Sens. Actuators, B,* 2013, **188**, 988-998.
12. F. Alatas, O. Alatas, M. Metintas, O. Colak, E. Harmanci and S. Demir, *Lung cancer*, 2001, **31**, 9-16.
13. W. Q. Bai, Y. Y. Wei, Y. C. Zhang, L. Bao and Y. Li, *Anal. Chim. Acta*, 2019, **1061**, 101-109.
14. B. R. Miller, T. Q. Wei, C. J. Fields, P. K. Sheng and M. Y. Xie, *RNA*, 2018, **24**, 1871-1877.
15. S. Cinti, E. Proietti, F. Casotto, D. Moscone and F. Arduini, *Anal. Chem.*, 2018, **90**, 13680-13686.
16. E. O. Blair and D. K. Corrigan, *Biosens. Bioelectron.*, 2019, **134**, 57-67.
17. T. T. Fan, Y. Du, Y. Yao, J. Wu, S. Meng, J. J. Luo, X. Zhang, D. Z. Yang, C. Y. Wang, Y. Qian and F. L. Gao, *Sens. Actuators, B,* 2018, **266**, 9-18.
18. H. B. Sun, Y. L. Qiu, Q. R. Liu, Q. W. Wang, Y. Huang, D. X. Wen, X. J. Zhang, Q. Y. Liu, G. D. Liu and J. M. Kong, *Biosens. Bioelectron.*, 2019, **131**, 193-199.
19. M. J. Shin and J. S. Shin, *Microchim. Acta*, 2020, **187**.
20. I. Isildak, F. Navaeipour, H. Afsharan, G. S. Kanberoglu, I. Agir, T. Ozer, N. Annabi, E. E. Totu and B. Khalilzadeh, *Microchim. Acta*, 2020, **187**.
21. X. C. Pan, S. Lathwal, S. Mack, J. J. Yan, S. R. Das and K. Matyjaszewski, *Angew Chem., Int. Ed.*, 2017, **56**, 2740-2743.
22. H. Qian and L. He, *Anal. Chem*., 2009, **81**, 4536-4542.
23. A. K. Sahu, S. Pitchumani, P. Sridhar and A. K. Shukla, *Bull. Mater. Sci*., 2009, **32**, 285-294.
24. P. G. Su, Y. L. Sun and C. C. Lin, *Sens. Actuators, B*, 2006, **115**, 338-343.
25. K. J. Peng, K. H. Wang, K. Y. Hsu and Y. L. Liu, *Acs Macro Lett.*, 2015, **4**, 197-201.
26. K. Feng, L. Liu, B. B. Tang, N. W. Li and P. Y. Wu, *ACS Appl. Mater.*, 2016, **8**, 11516-11525.
27. K. J. Peng, J. Y. Lai and Y. L. Liu, *Rsc Adv.*, 2017, **7**, 37255-37260.
28. K. Matyjaszewski and J. Xia, *Chem. Rev.*, 2001, **101**, 2921-2990.
29. C. M. Li, J. Yang, P. Y. Wang, J. Liu and Q. H. Yang, *Microporous Mesoporous Mater.,* 2009, **123**, 228-233.
30. Q. Hu, Q. W. Wang, J. M. Kong, L. Z. Li and X. J. Zhang, *Biosens. Bioelectron.*, 2018, **101**, 1-6.
31. Y. Li, W. K. Xu, X. R. Zhao, Y. F. Huang, J. J. Kang, Q. Qi and C. L. Zhong, *Analyst*, 2018, **143**, 5094-5102.
32. N. V. Tsarevsky, T. Pintauer and K. Matyjaszewski, *Macromolecules*, 2004, **37**, 9768-9778.
33. M. Fantin, F. Lorandi, A. Gennaro, A. A. Isse and K. Matyjaszewski, *Synthesis-Stuttgart*, 2017, **49**, 3311-3322.
34. J. C. Dai, Y. C. Dong, C. Yu, Y. X. Liu and X. G. Teng, *J. Membr. Sci.*, 2018, **554**, 324-330.
35. P. Chmielarz, M. Fantin, S. Park, A. A. Isse, A. Gennaro, A. J. D. Magenau, A. Sobkowiak and K. Matyjaszewski, *Prog. Polym. Sci*., 2017, **69**, 47-78.
36. Q. Hu, X. B. Deng, J. M. Kong, Y. Y. Dong, Q. R. Liu and X. J. Zhang, *Analyst*, 2015, **140**, 4154-4161.
37. B. C. Zhu and J. Travas-Sejdic, *Analyst*, 2018, **143**, 687-694.
38. S. M. R. Niya and M. Hoorfar, *J. Power Sources,* 2013, **240**, 281-293.
39. Q. Hu, Q. W. Wang, C. H. Jiang, J. Zhang, J. M. Kong and X. J. Zhang, *Biosens. Bioelectron.*, 2018, **110**, 52-57.
40. N. Samadi and S. Narimani, *Anal. Bioanal. Chem. Res.,* 2019, **6**, 47-57.
41. Z. Guo, Q. Niu, Q. Yang, T. Li and H. Chi, *Anal. Chim. Acta*, 2019, **1065**, 113-123.
42. P. H. Lepage, R. Peytavi, M. G. Bergeron and M. Leclerc, *Anal. Chem.*, 2011, **83**, 8086-8092.
43. H. G. Chen, W. Ren, J. Jia, J. Feng, Z. F. Gao, N. B. Li and H. Q. Luo, *Biosens. Bioelectron.*, 2016, **77**, 40-45.
44. M. Liu and B. X. Li, *Microchim. Acta*, 2016, **183**, 897-903.